Available online at www.sciencedirect.com
SCIENCE DIRECT®
Tectonophysics 371 (2003) 223–241
TECTONOPHYSICS
www.elsevier.com/locate/tecto

Morphological and structural relations in the Galilee extensional domain, northern Israel

A. Matmon[a,b,*], S. Wdowinski[c], J.K. Hall[b]

[a] Department of Geology, Hebrew University, Jerusalem 91904, Israel
[b] Geological Survey of Israel, 30 Malkhe Yisrael Street, Jerusalem 95501, Israel
[c] Department of Geophysics and Planetary Sciences, Tel Aviv University, Tel Aviv, 69978, Israel

Received 6 December 2001; accepted 11 June 2003

Abstract

The Lower Galilee and the Yizre'el Valley, northern Israel, are an extensional domain that has been developing since the Miocene, prior and contemporaneously to the development of the Dead Sea Fault (DSF). It is a fan-shaped region bounded in the east by the N–S trending main trace of the DSF, in the north by the Bet-Kerem Fault system, and in the south by the NW–SE trending Carmel Fault. The study area is characterized by high relief topography that follows fault-bounded blocks and flexures at a wavelength of tens of km. A synthesis of the morphologic–structural relations across the entire Galilee region suggests the following characteristics: (1) Blocks within the Lower Galilee tilt toward both the southern and northern boundaries, forming two asymmetrical half-graben structures, opposite facing, and oblique to one another. (2) The Lower Galilee's neighboring blocks, which are the Upper Galilee in the north and the Carmel block in the southwest, are topographically and structurally uplifted and tilted away from the Lower Galilee. (3) The southern half-graben, along the Carmel Fault, is topographically and structurally lower than the northern one. Combining structural and geological data with topographic analysis enables us to distinguish several stages of structural and morphological development in the region. Using a semi-quantitative evolutionary model, we explain the morpho-structural evolution of the region. Our results indicate that the Galilee developed as a set of two isostatically supported opposite facing half-grabens under varying stress fields. The southern one had started developing as early as the early Miocene prior to the formation of the DSF. The northern and younger one has been developing since the middle Pliocene as part of the extension process in the Galilee. Elevation differences between the two half-grabens and their bounding blocks are explained by differences in isostatic subsidence due to sedimentary loading and uplift of the northern half-graben due to differential influences of the regional folding.

Keywords: Tilted blocks; Normal faults; Galilee; Rift margins; Extension

1. Introduction

The Galilee region is located in northern Israel between the Mediterranean and the Dead Sea Fault (DSF), which is the boundary separating between the Sinai and Arabian plates (Garfunkel, 1970, 1981; Fig. 1). The present structure of the Galilee has been

* Corresponding author. Current address: U.S. Geological Survey, 345 Middlefield Road MS #977, Menlo Park, CA, 94025, USA.
E-mail address: amatmon@usgs.gov (A. Matmon).

0040-1951/03/$ - see front matter © 2003 Elsevier B.V. All rights reserved.
doi:10.1016/S0040-1951(03)00237-3

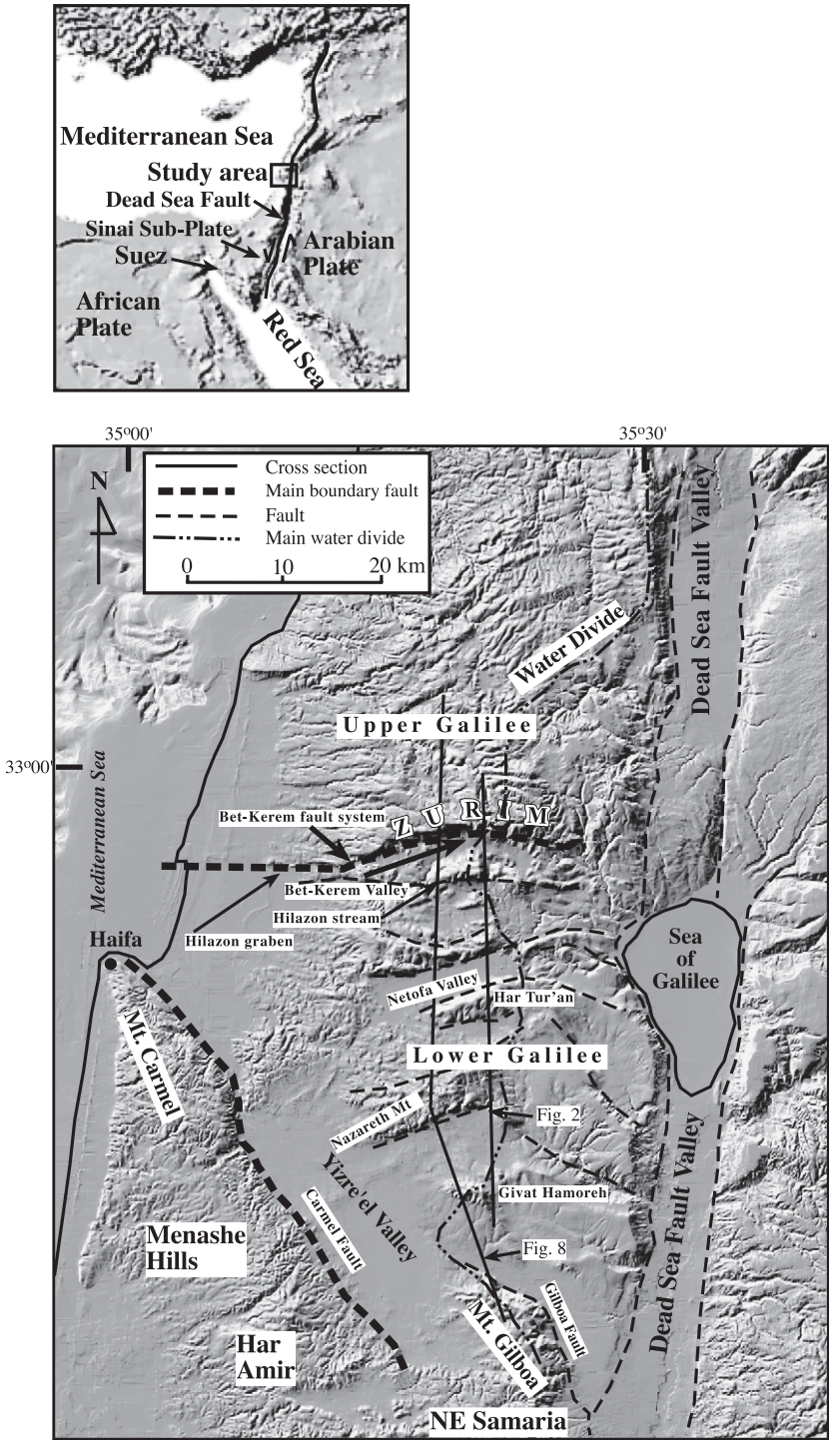

Fig. 1. General location map (Israel grid). Database: Hall (1993, 1996). Inset: eastern Mediterranean tectonic setting. Dead Sea Faults (thin dashed lines) are drawn schematically.

developing since the Miocene, prior and contemporaneously to the development of the DSF (Freund, 1970). Understanding the development and evolution of the Galilee provides important observations regarding the tectonic and structural conditions that existed in the region prior, during, and after the formation of the DSF. Furthermore, the Galilee is the only extensional domain that extends well beyond the Dead Sea Fault's narrow rift margins. Hence, studying the structural and morphological relations between the Galilee and the Dead Sea Fault provide better understanding of the coupling between transcurrent movements and adjacent diffuse extensional deformation. Such extensional domains are also observed along other continental transform faults, e.g., the Gadiz and Buyuk Menderes grabens in western Turkey south of the North Anatolian Fault.

The Galilee is divided into two major domains, the Lower and Upper Galilee (Fig. 1). The study area (which includes the Lower Galilee and the Yizre'el Valley) consists of a series of E–W trending ridges and tilted blocks bounded by normal faults (Freund, 1970) and separated by elongated valleys (Figs. 1 and 2). The study area is bounded in the north by the Upper Galilee block that rises above the Zurim Escarpment and in the south by the Carmel block (Fig. 1). Because the northern and southern boundaries are oblique to each other (Fig. 1), the extended region has a fan shape. It is about 50 km wide at its eastern side (close to the DSF) and narrows towards the west to about 20 km along the coastal plain.

The topographic–structural relations in the Galilee have been studied for almost four decades. The relations between Miocene and Pliocene structures and topography were studied by analyzing sedimentary sequences (Kafri and Ecker, 1964; Issar and Kafri, 1972; Shaliv, 1991). Fruend (1970), Ron et al. (1984), and Ron and Eyal (1985) studied the Neogene tectonic activity and stress fields in the Galilee and pointed out the correlation between topography and young structural elements. Freund (1965) related the extension in the Galilee to the left lateral displacement and geometry of the DSF and calculated that such extension amounted to 5–7% (Freund, 1970). While Freund's suggestion that left lateral movement along the DSF explains the extension and some other morphologic and structural features in the Galilee, it does not provide answers to other observation, mainly the structural and topographic characteristics of the bounding blocks of the Lower Galilee.

In this study, we systematically explore and characterize the relations between topography and structure in the Lower Galilee and Yizre'el Valley and their bounding blocks. Our study expands beyond the extensional Lower Galilee and Yizre'el Valley, and includes the neighboring Upper Galilee and Carmel blocks. The southwestern boundary of the extensional domain is well defined by a single fault, the Carmel Fault. However, the southeastern boundary is not as well defined. It diffuses into several parallel faults, which form the northeastern Samaria and the Gilboa blocks. We exclude these areas from our analysis for several reasons: the complexity of the boundary fault, the influence the Dead Sea Fault Valley marginal normal faults on the eastern blocks, and the lack of structural data from the NE Samaria.

We first provide the geological background of the region and describe its main structural and morphological elements. Then, we analyze the Galilee's morpho–tectonic relations by constructing arc-shaped sections across the fan-shape extensional domain and its neighboring uplifted blocks. Our analysis results combined with previous observations suggest that the morphologic and tectonic history of the Lower Galilee, the Yizre'el Valley, and their adjacent bounding blocks are best described by a set of two opposite facing half-grabens, a southern one that started developing as early as the early Miocene and a northern and younger one that has been developing since the middle Pliocene. The observed relations between the structure and topography are explained by using a semi-quantitative evolutionary model.

2. Geologic background

The structure and recent topography did not evolve contemporaneously throughout the Galilee. Its various parts experienced different geological histories. A pre-Eocene structure, the Syrian Arc fold belt (Krenkel, 1924; Picard, 1943), which in the Galilee consists of a series of N–S oriented anticlines and synclines, started developing in the Senonian as a response to closing of the Tethys Ocean (Flexer et al., 1970). The Syrian Arc fold belt does not influence the present morphology of the Galilee. Here we provide a short review of the

geological history of the region from the late Eocene to the late Pliocene, which is also summarized in Table 1.

Prior to the late Eocene, the Galilee region was a part of a continental shelf that accumulated mainly carbonate sediments. The regression of the Tethys Ocean at the end of the Eocene and the slow uplift of the land left behind a flat exposed plain underlain by Eocene carbonate units. This plain drained westward through a regional drainage system (Picard, 1943, 1951; Garfunkel and Horovitz, 1966; Nir, 1970; Garfunkel, 1988; Avni, 1990, 1991; Zilberman, 1992; Garfunkel and Ben-Avraham, 1996; Begin and Zilber-

Table 1
Summary of landscape development in the Galilee

Stage	Time	Dead Sea Fault Valley	Carmel Fault line	Lower Galilee	Zurim Escarpment	Upper Galilee
1	Late Eocene to early Miocene	Global sea regression, extensive erosion and formation of erosional plain (e.g., Garfunkel, 1988)				
2	Early Miocene to middle Miocene	Development and fill of local basins. Compatible sedimentation and tectonic rates.				
		Left lateral motion along Dead Sea Fault (Garfunkel, 1981).	Initial subsidence of Yizre'el Valley and accumulation of volcanics and sediments. Initial relief.			
3	Middle Miocene to early Pliocene	Tectonic quiescence, some erosion and deposition in local basins.				
		Strike slip movement, subsidence and accumulation of sediments and volcanics	Slow subsidence of Yizre'el Valley. Strike-slip faulting	Faulting (normal and strike-slip) and development of initial relief. Some strike slip faults might have been active earlier under Syrian Arc stress field.	Initial relief of Zurim Escarpment	Faulting (normal and strike-slip) and development of initial relief
		Continuation of strike slip movement, subsidence of Jordan Valley	Erosion of Miocene relief	Erosion of relief	Erosion of Miocene relief	Erosion
4	Early Pliocene to early Pleistocene	Normal faulting along the Dead Sea Fault boundaries (Heimann, 1990; Hurwitz et al., 2002)	Reactivation as normal fault and development of recent relief	Extensive normal faulting and development of recent relief	Development of recent relief	Development of relief along major faults (Matmon et al., 2000)
5	Early Pleistocene to recent	Strike slip movement (e.g., Marco et al., 1997)	Continuation of normal faulting at slow rates.	Continuation of normal faulting at slow rates. Arching and formation of main water divide (Matmon et al., 1999).	Continuation of normal faulting at slow rates.	Continuation of normal faulting at slow rates. Arching and formation of main water divide.

Unless noted otherwise, data from Shaliv (1991, and references therein), Kafri and Ecker (1964), Issar and Kafri (1972).
Stage numbers correspond to geological stages in text.

man, 1997). By early Miocene, a regional erosional plain dominated the topography of the area (Picard, 1943; Garfunkel, 1970, 1978) (Table 1, stage 1).

Miocene to recent tectonic movements have deformed the Oligocene erosional plain. The earliest stages of extension in the Galilee took place in its southern part along the Carmel Fault and the Yizre'el Valley. The Yizre'el Valley is the largest and deepest among the series of Lower Galilee basins and consists of a thick Neogene sedimentary and volcanic sequence (e.g., Schulman, 1959, 1962; Shaliv, 1991). During the Miocene, initial relief along the Carmel Fault was formed (Table 1, stage 2; Karcz, 1959; Achmon, 1986; Shaliv, 1991; Kashai and Picard, 1958). From the early Miocene to the early Pliocene, lateral displacements took place along NW and NE trending faults through the entire Galilee. However, the topographic expression of most of this activity was eroded (Matmon et al., 2000). The Carmel Fault was also activated as a strike-slip fault during the later part of this period (Table 1, stage 3; Ron et al., 1984).

Starting in the middle to late Pliocene, widespread volcanism occurred mainly in the eastern Lower Galilee (Shaliv, 1991). Normal faulting that formed most of the structures controlling the recent morphology of the Lower Galilee followed this volcanic stage. Older faults, such as the Carmel Fault, were reactivated to form their present morphology (Table 1, stage 4). The development of a broad structural arch formed the mountainous backbone of Israel between the Mediterranean and the DSF and continued through the Pleistocene (Table 1, stage 5; Matmon et al., 1999). The southward tilted sediments within the fill of the Yizre'el Valley which thicken towards the Carmel Fault, suggest continuous motion along the fault during the Neogene and the quaternary (Kafri and Ecker, 1964). A similar situation exists in the down faulted block (the Hilazon graben) along the western end of the Bet-Kerem Fault system. However, the Hilazon graben contains only Quaternary sediments, indicating that the graben started subsiding later than the Yizre'el Valley.

The N–S extensional deformation in the Galilee has continued through the Quaternary (Table 1, stage 5). Displaced Pleistocene basalts indicate normal displacement along some faults in the eastern Upper Galilee (Mor et al., 1987). Fresh fault scarps are exposed in several locations at the foot of uplifted blocks in the Galilee and suggest major pulses of normal displacement during the Holocene (Gran-Mitchel et al., 2001). Hanging and truncated valleys along some Galilee escarpments (Nir, 1970) also suggested quaternary uplifting.

3. Structure and morphology

3.1. Structure

Two N–S trending structural systems affect the morphology of the Galilee. The first is the Dead Sea Fault that bounds the Galilee in the east; it consists of left-lateral faults, separating the Arabian plate from the Sinai sub-plate (Garfunkel, 1970; Fig. 1) and a series of normal faults, which form escarpments bounding a narrow rift valley. The activity along the rift's faults has been continuous since the Miocene to the present (Quennell, 1959; Garfunkel, 1981, 1988; Heimann, 1990; Belitzki, 1997; Marco et al., 1997; Ellenblum et al., 1998). The second N–S trending structural system is a broad arch, 40–60 km wide, bounded between the Mediterranean and the DSF. In the Galilee, the amplitude of the arch, which took place during the Pleistocene, is 200–300 m (Matmon et al., 1999). A number of researchers, working in different areas along the western margins of the DSF, concluded that the development of the broad structural arch is related to that of the DSF (Picard, 1943; Bentor and Vroman, 1951, 1961; Ball and Ball, 1953; Salamon, 1987; ten Brink et al., 1990; Wdowinski and Zilberman, 1996, 1997; Matmon et al., 1999).

The Carmel Fault, which is the southern boundary of the Lower Galilee, was formed in the early Miocene (Shaliv, 1991; Kashai and Picard, 1958) and has been active ever since (Hofstetter et al., 1996; Salamon et al., 1996). The western part if the Carmel Fault is defined by a single fault. To the east, the Carmel Fault splays into a series of E–W trending normal faults which extend to the Dead Sea Fault valley and form the extensional domain of northeast Samaria which is bounded between the Gilboa and Fari'a Faults. Some studies suggest that a weak zone existed along the Carmel area since the late Paleozoic, although it did not correspond directly with the present location of the Carmel Fault (e.g., Garfunkel and Derin, 1984; Garfunkel and Almagor, 1985; Achmon, 1986; Dvorkin

and Kohn, 1989; Ben-Gai and Ben-Avraham, 1995; Achmon and Ben-Avraham, 1997). The activity along the Carmel Fault predated the activity of the DSF and the adjacent Yizre'el Valley was formed as one in a series of basins associated with the opening of the Red Sea (Shaliv, 1991). The Carmel Fault truncates the preexisting syncline (Menashe Hills) and anticline (Mt. Carmel and Har Amir) structure of the Syrian Arc Fold Belt (Picard and Golani, 1965). The topographic expression of the Carmel Fault is dominant where the fault crosses the anticlines and poor where it crosses the syncline. Geologic and topographic considerations as well as recent seismic activity imply both normal and lateral displacements along the Carmel Fault (Hofstetter et al., 1996; Salamon et al., 1996).

Two major fault systems are identified within the Galilee: strike-slip faults oriented NW–SE and NE–SW (Freund, 1970; Ron et al., 1984; Ron and Eyal, 1985) and E–W oriented normal faults forming most of the Galilee's morphology. The shallow structure of the Lower Galilee and its morphology are dominated by E–W oriented tilted blocks, half-grabens, grabens and horsts (Fig. 2; Schulman, 1962; Kafri and Ecker, 1964; Issar and Kafri, 1972; Mero, 1983; Sivan, 1996; Sivan et al., 1999). E–W normal faults are less dominant in the Upper Galilee and control the morphology only at the eastern and western edges of the area. The Upper Galilee is intensively deformed by the NW–SE and NE–SW strike-slip fault systems, although these do not contribute to its recent morphology.

3.2. Morphology

The unique morphology of the Galilee is best observed by tracing the water-divide between the Mediterranean and the rift valley of the DSF. The drainage system in Israel is composed of eastern and western basins, which are drained to the rift valley and the Mediterranean, respectively (Fig. 3). The main water divide between these two base levels is located along the mountainous backbone of Israel which is oriented N–S and is parallel to sub-parallel to the DSF. The mountainous backbone was formed as a result of the development of the broad structural arch between the DSF and the Mediterranean since the Pliocene. The typical flat and low relief surface of the mountainous backbone is generally composed of Mesozoic carbonate rocks of the Judea Group and might reflect the uplifted Oligocene to early Miocene erosional plain (Garfunkel, 1988). The summits of the major mountainous regions (the Negev, Judea, Samaria, and Upper Galilee) are uplifted to a similar elevation of 900–1000 m above sea level (Fig. 3).

The uniform topography of the mountainous backbone along the western margins of the DSF is truncated in the domain that includes the Lower Galilee and northeastern Samaria. In this region, the mountainous backbone was subjected to N–S extension that formed the series of elongated ridges and valleys perpendicular to the axis of the main water divide. The summits of the Lower Galilee are 400–500 m lower compared to the other mountain ridges in Israel (Fig. 3). However,

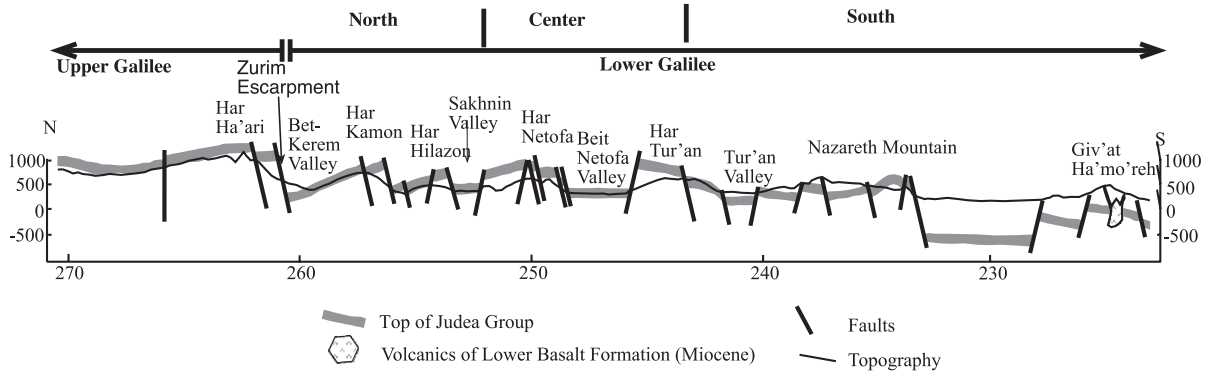

Fig. 2. The shallow structure of the Galilee (after Freund, 1970). The northern part of the Lower Galilee is composed of blocks tilted to the north and the southern part of blocks tilted to the south. The central part is dominated by horsts.

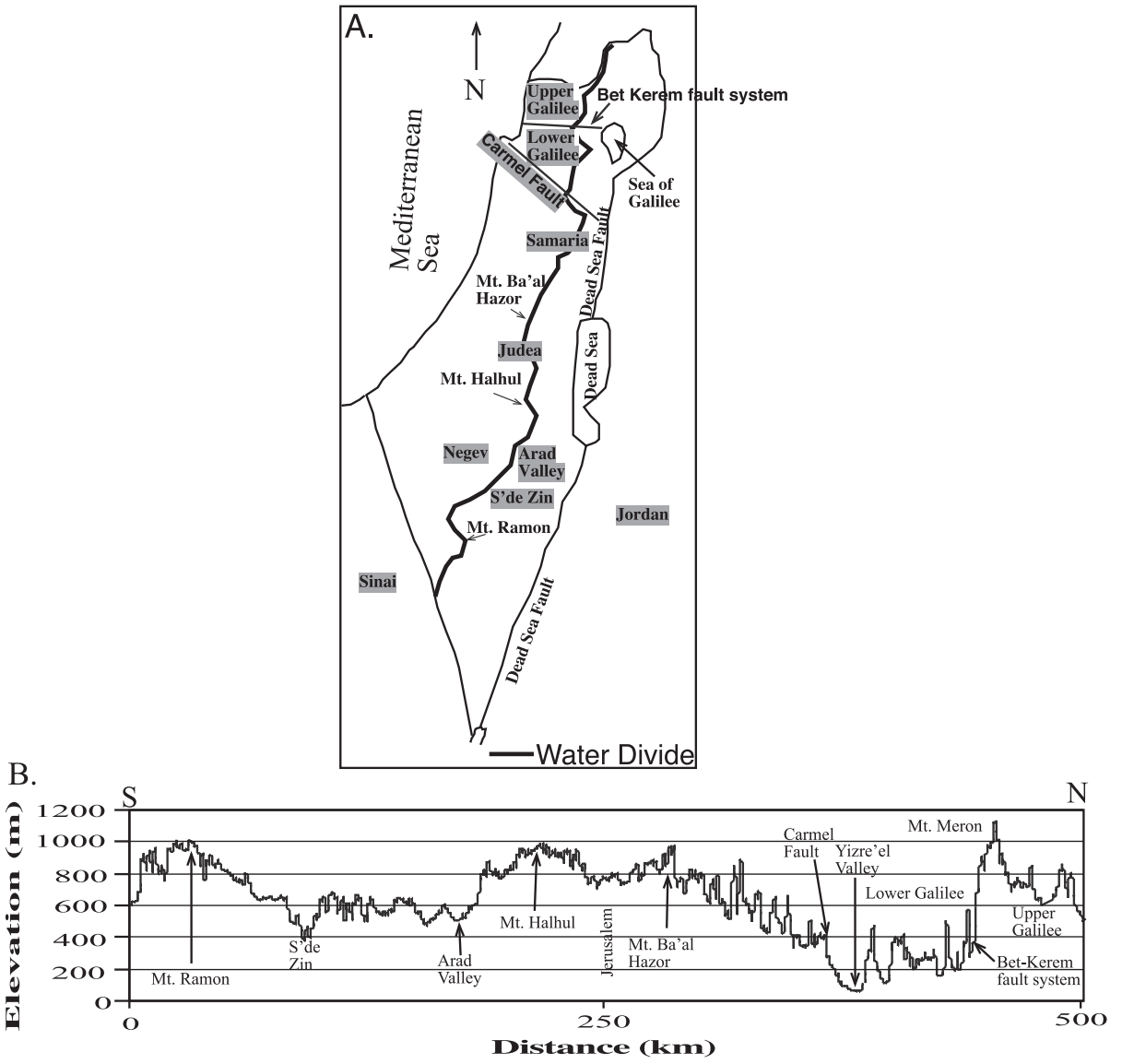

Fig. 3. (A) Map showing the main water-divide that separates the western margins of the Dead Sea Fault into the two principle watersheds: the Dead Sea Fault Valley and the Mediterranean. The water divide is parallel to subparallel to the Dead Sea Fault Valley and is located on the central mountainous backbone of Israel. Dead Sea faults are drawn schematically. (B) Topographic profile along the main water-divide. The altitude of the summits of most of the mountain ranges along the water-divide is 900–1000 m above sea level. The Lower Galilee is the lowest mountainous region with its summits rising up to an altitude of 500–600 m above sea level. The lowest points along the water divide are also located in the Lower Galilee.

The stratigraphic units exposed on top of the uplifted structures in the Lower Galilee are identical to those exposed in other mountainous structures in Israel. Therefore, it is reasonable to assume that the area was not structurally low before the Oligocene–Miocene denudation and it probably experienced the same level of denudation as the other mountainous structures during that time. The lowest points along Israel's main water divide are located in the Lower Galilee, in which the lowest one is in the Yizre'el Valley at an

elevation of 70 m above sea level (Fig. 3). The greatest structural relief (relief formed by faulting as opposed to relief formed by surface processes), up to 700 m, is found in the Lower Galilee, where changes between low and high regions are most abundant.

4. Morpho-structural analysis

The Lower Galilee and the Yizre'el Valley are a fan-shaped extensional domain, bounded by two fault systems, the Carmel Fault and Bet-Kerem Fault system, which are oblique to one another. In order to understand the regional scale structural and morphological relations between the extending region and its neighboring blocks, we use arc-shaped geological cross-sections, which are drawn normal to both major fault systems. The arc-shaped sections are also parallel to the regional average dip of the NW-tilting Upper Galilee and the WSW-tilting Carmel block (Fig. 4). Thus, unlike in previous studies (e.g., Kafri and Ecker, 1964; Freund, 1970; May, 1987), which drew structural sections in one direction across one of the structural elements, our cross-sections display the entire structure of the Lower Galilee, the Yizre'el Valley, and their structural boundaries. The focus of the arcs was determined at the crossing point between the extrapolation of the Carmel Fault and the Bet-Kerem Fault system westward into the Mediterranean (Fig. 4). Twelve cross-sections were constructed at a spacing of 4 km. All cross-sections initiate in the Upper Galilee, cross the Lower Galilee, and terminate west to south west of the Carmel line. We include in our analysis only cross-sections 1–9, which cross the well-defined Carmel Fault (Fig. 4).

Topographic and structural data were plotted together to allow direct comparison between the morphology and structure of the region (Fig. 5). Topographic data were obtained using the Digital Terrain Model of Israel with a 25-m grid and 10-m vertical resolution (Hall, 1993, 1996). Structural data, based on top Judea Group datum, was determined from previous works (Golani, 1957; Saltzman, 1964; Eliezri, 1965; Glikson, 1966; Kafri, 1972; Levy, 1983; May, 1987; Cohen, 1988) and marked along each arc at 5-km spacing. This spacing enabled the detection of only the major faults and folds that control the structure of the Galilee and filter out small and local scale structures. Thus, most of the faults within the Lower Galilee are not expressed in the cross-sections and the emphasis is put on the boundary faults. The precision in determining the structural elevation is influenced by two error sources: original errors in structural maps and the interpolation process. Original errors in mapping are assumed to be random. In structural maps with 50- or 100-m contours the interpolation process might cause errors up to ± 50 or ± 100 m, respectively. These errors are small compared to the amount of displacement that ranges between 600 and 1300 m along the main faults in the Galilee and up to 2000 m along the Carmel Fault. Thus, we estimate the total uncertainty in structural elevations in the range of 100 m.

Here, we present only three cross-sections (3, 7, and 9; Figs. 4 and 5), which represent the western, central, and eastern parts of the Galilee, respectively. Section 3 shows an almost symmetrical morphology across the extending region. The sedimentary fill of the Yizre'el Valley in the south and the similar elevations of both escarpments at these locations result in the symmetric topography. Two escarpments bound the low elevation morphology of the Lower Galilee: the northern one (Zurim Escarpment) formed by the Bet-Kerem Fault system and the southern one formed by the Carmel Fault. From the top of both escarpments, the topography and structure subside toward the Mediterranean. Unlike the symmetric topography, the structure in section 3 is asymmetric, in which the Lower Galilee subsides to the south to form the deep half-graben of the Yizre'el Valley. The southern half-graben, which forms the Yizre'el Valley dips sharply towards the Carmel Fault. In section 7, both the morphology and structure appear asymmetric. The low morphology of the Carmel results from the synclinal structure of the uplifted block crossed by the section line. The topography and structure subside from the Lower Galilee boundaries towards the Mediterranean. Both the northern and the southern half-grabens dip towards their respective bounding fault. In section 9, the morphology of the uplifted Upper Galilee dips towards the Lower Galilee; an escarpment does not define the boundary between the Upper and Lower Galilee. However, the structure presents similar characteristics to those seen in the previous cross-sections.

A synthesis of the three sections presented above (and of the other unpresented sections) suggests the

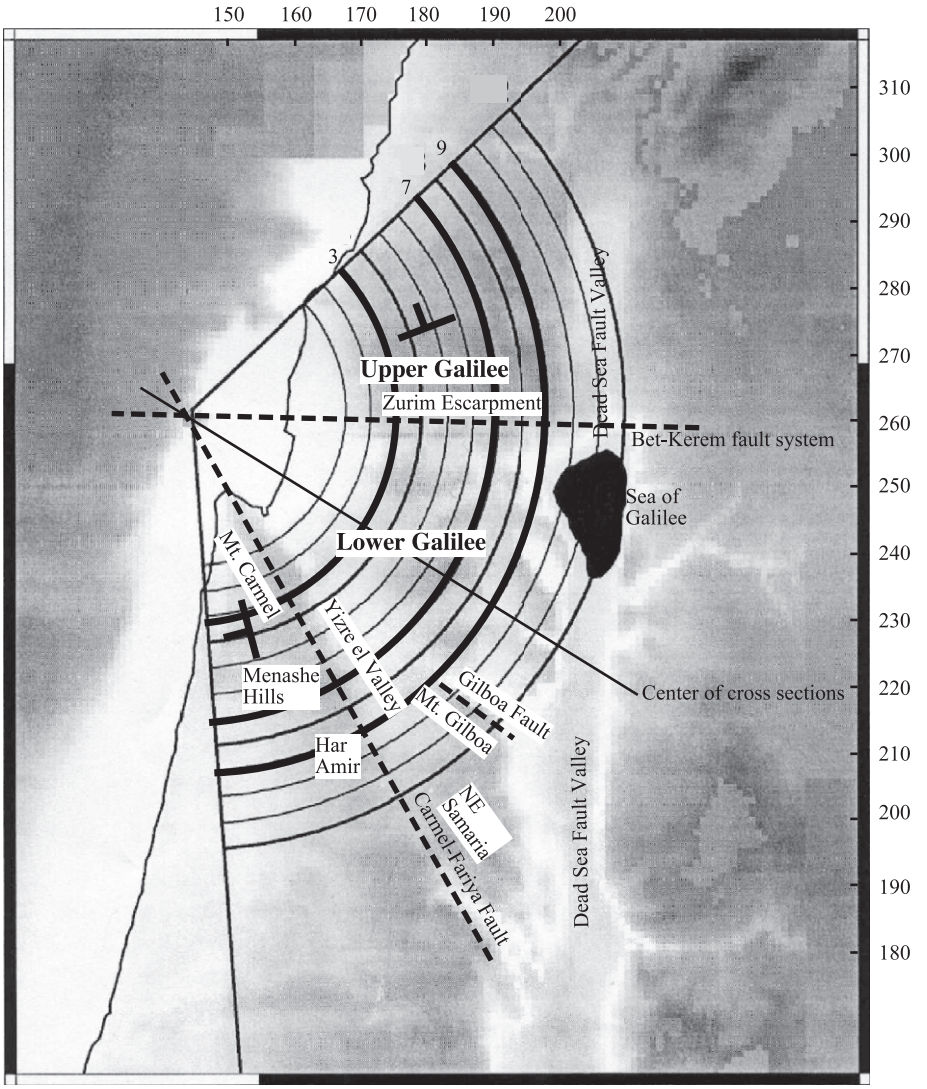

Fig. 4. Location of topographic and structural profiles (Israel grid). Dashed lines—the general trace of the Carmel Fault line and the Bet-Kerem Fault system. Solid lines—NW and SW limits of profiles. Regional tilt of the Upper Galilee and Carmel blocks is marked by thick plus signs. To avoid dip measurements of internally deformed units, dip measurements were taken from a minimum distance of 10 km from the escarpments and from hard Cenomanian and Turonian limestone and dolomite units. The cross-sections were constructed along arched lines to intersect the Bet-Kerem and Carmel Fault at right angles and to coincide with the regional tilt of the Upper Galilee and Carmel blocks.

following characteristic of the Galilee's morphology and structures: the Carmel Block and the Upper Galilee are structurally high. Above the escarpments, structure and topography subside towards the Mediterranean. The Carmel Block is tilted to the WSW; the Upper Galilee Block is tilted to the NW (Fig. 4). The structure across the extending domain of the Lower Galilee and Yizre'el Valley shows a distinct asymmetry, in which the southern half-graben, which forms the Yizre'el Valley, is structurally 600–1600 m and topographically ~ 300 m lower than the northern half-graben which forms the Bet-Kerem Valley (Fig. 5). The Carmel block is topographically ~ 500 m lower than the Upper Galilee. The top of Zurim Escarpment is several hundreds of meters structurally higher than

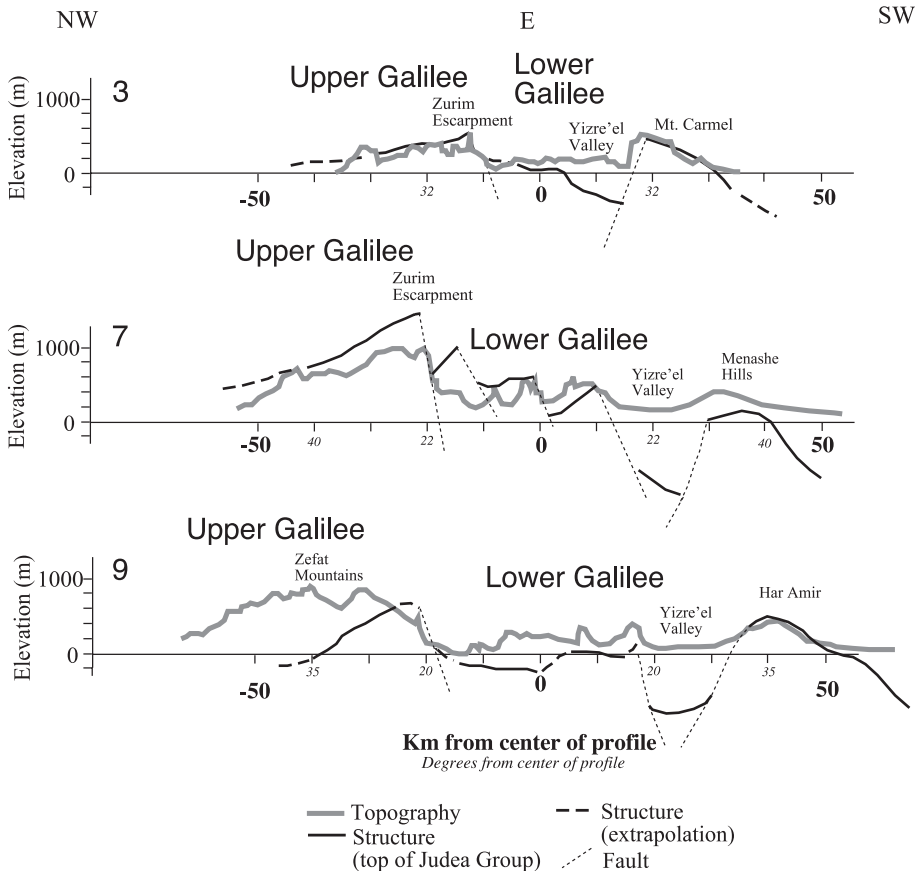

Fig. 5. Topographic and structural sections along lines indicated in Fig. 4. Cross-sections 3, 7, and 9 represent the western, central and eastern parts of the Galilee, respectively. For details, see text.

the Carmel block. Both bounding blocks are structurally higher than their adjacent valleys. However, because the base of the Lower Galilee rises from south to north and inner Lower Galilee deformation consists of uplifted blocks, there are a few summits in the Lower Galilee that are topographically and structurally higher than the Carmel.

The two bounding faults, the Carmel Fault and the Bet-Kerem Fault are characterized by a distinct structural asymmetry (Fig. 5), forming half-graben structures. The Carmel Fault has a more developed "classical" half-graben structure, in which a single boundary fault separates between the uplifted Carmel Block and the downward tilted Yizre'el Valley. The Bet-Kerem Fault separates between the uplifted Upper Galilee block and the subsided northern Lower Galilee block, which is transected by synthetic and antithetic normal faults forming a series of ridges and valleys.

5. Model

The Galilee's structure and morphology are complex. They reflect an accumulated contribution of deformation episodes and surface processes that have occurred in the region since the early Oligocene. We present here a semi-quantitative evolutionary model that explains the formation and evolution of the Galilee's structure and morphology. The model considers the contribution of four regional-scale processes: formation of a regional erosional plain, half-graben formation, isostatic vertical movements, and regional-flexure (arching). Some of the processes occur simul-

taneously during the slow and long development (millions of years) of a fault system. Before presenting the model, we provide a short description of each the four processes that shaped the Galilee's structure and morphology.

5.1. Geodynamic and morpho-structural processes

5.1.1. Formation of a regional erosional plain

The regression of the Tethys Ocean at the end of the Eocene was followed by the development of a westward to northwestward flowing regional drainage system (Picard, 1943, 1951; Garfunkel and Horovitz, 1966; Nir, 1970; Garfunkel, 1988; Avni, 1990, 1991; Zilberman, 1992; Garfunkel and Ben-Avraham, 1996; Begin and Zilberman, 1997). The truncation of the Eocene carbonate units by the drainage system, exposed the hard limestone and dolomite of the Syrian Arc anticlines and the soft chalks of the Syrian Arc synclines. There is no geologic evidence to indicate high relief at that time, and it is reasonable to assume that uplift and denudation rates were equal and a low relief landscape was maintained.

5.1.2. Half-graben formation

Extensive research conducted in various continental extensional domains has shown that in many of the extensional systems, the extension is governed by simple shear deformation in the upper crust (e.g., Wernicke, 1981; Wernicke and Burchfield, 1982; Ebinger et al., 1987; Rosendahl, 1987). In narrow extensional regions, such as continental rifts, the simple shear extension is expressed by half-graben

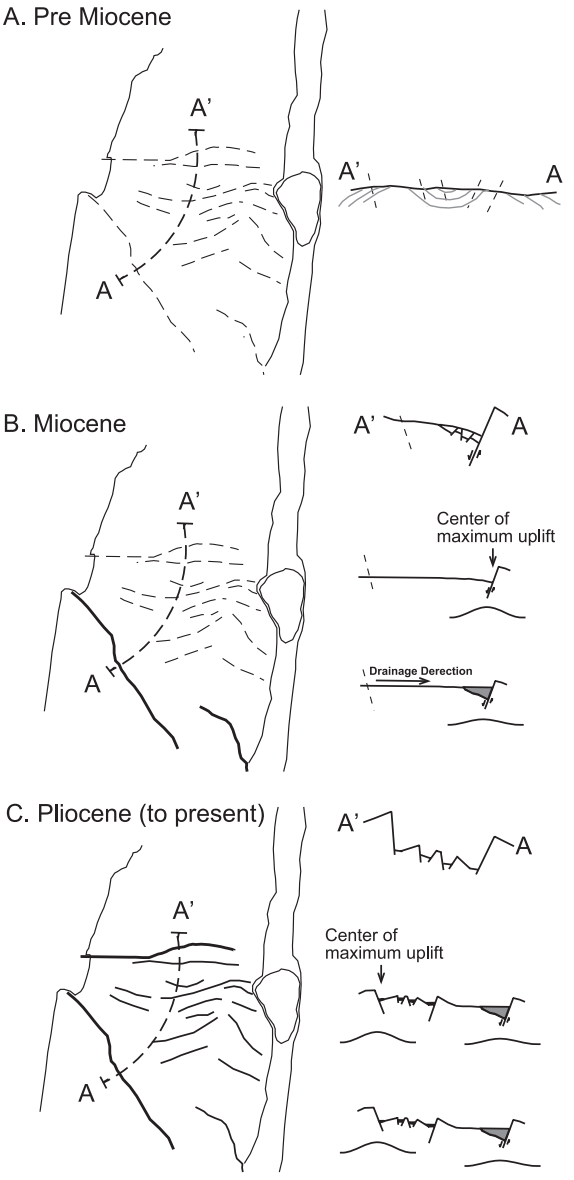

Fig. 6. Time evolution of the Galilee. Thick solid lines—Major boundary faults. Thin solid lines—secondary faults. Dashed lines—future location of faults. Shaded areas in cross-sections—sedimentary and volcanic fill. (A) Pre-Miocene: low relief terrain dominated the topography following the development during the Oligocene of an erosional plain. Cross-section on right shows topography (black line) and truncated pre-Eocene structure (gray lines). (B) Miocene: the formation of the Carmel Block along the Carmel Fault and the development of the southern half-graben. Top cross-section shows the structure of the half-graben unit. Location of center of isostatic uplift due to normal faulting is shown in the middle cross-section. Following the formation of the half-graben, drainage systems developed and transported sediment from north to south. Sediments and volcanics accumulated in the half-graben, and the isostatic uplift was reduced as demonstrated by the less arched line below the right side of the lower cross-section. Notice that the topography of the Lower Galilee tilts to the south into the Yizre'el Valley. (C) Pliocene to recent: the formation of the Bet-Kerem Fault system and the northern boundary of the Lower Galilee. Inner Lower Galilee structures were formed at this stage as well. Upper cross-section shows schematic structure of the region. The arched line below the left side of the middle cross-section demonstrates Isostatic compensation. Because there is very little sedimentary fill in the northern valleys, there is no subsidence due to sedimentary loading. Arching of the western margin of the Dead Sea Fault uplifts the northern half-graben (lower cross-section). This structural arch does not affect the southern half-graben because it lies west of the arching axis.

structures (e.g., Ebinger et al., 1987; Rosendahl, 1987; Ebinger, 1989; Wdowinski and Zilberman, 1996, 1997).

5.1.3. Isostatic vertical movements

Isostatic uplift and subsidence occur in response to changes of rock load within the lithosphere or other mass load (mostly ice or water) above the lithosphere. In extensional regions, crustal thinning reduces the lithospheric rock load causing local or regional isostatic uplift. The isostatic uplift of the extended region forms a distinguished morphology, which consists of an outward tilted elevated footwall adjacent to an inward tilted structural basin. A well-defined escarpment often marks the transition between the elevated footwall and the nearby basin. Loading of sediment in the basins causes the opposite effect of subsidence.

5.1.4. Regional-flexure (arching)

The arching of the western margins of the DSF has been mentioned and discussed by previous authors (Picard,1943; Bentor and Vroman, 1951, 1961; Salamon, 1987; Wdowinski and Zilberman, 1996). Some authors estimated an arching of about 200–400 m (Ball and Ball, 1953; Salamon, 1987; Matmon et al., 1999). ten Brink et al. (1990) pointed out the relationship between the rift axis isostatic compensation and the topography at the rift's margins. This type of arching has been observed in other rifts as well (e.g., East African Rift, Rosendahl, 1987; Ebinger, 1989). Wdowinski and Zilberman (1996) explained the arching formation as bending (in contrast to buckling that produces folds under compression) in response to the formation of the Dead Sea Rift. They attributed the broad fold structure to three processes: (1) regional pre-extensional westward strata deposition, (2) local (20–40 km wide) eastward tilt of the rift's western margins, which is the subsided block of the rift's half-graben structure, and (3) broad (100 km wide) isostatic uplift along the Dead Sea Rift. In this study, we do not attempt to quantify the arching, but rather use observed values.

Table 2
Relative elevation contributions of morphologic and geodynamic processes in the Galilee

Stage	Time	Process	Line force (Nm^{-1})	Elevation (m) Bet-Kerem structure	Elevation (m) Carmel structure	Note
1	Late Eocene to early Miocene	Formation of erosional plain (e.g., Garfunkel, 1988)		0	0	
2	Early Miocene to early Pliocene	Formation of the Carmel half-graben structure.	$1.7–2.0 \times 10^{11}$	0	300–350	Isostatic uplift due to tectonic unloading
3	Early Miocene to early Pliocene	Subsidence of Yizre'el Valley and accumulation of volcanics and sediments.	$-(0.8–1.0 \times 10^{11})$	0	−(150–175)	Isostatic subsidence due to sedimentary loading
4	Early Miocene to early Pliocene	Formation of a drainage system that flows from north to south into the Yizrer'el Valley (Kafri, 1997)		100–200	0	Elevation differences due the development of the Yizre'el Valley as base level. Assuming 0.5% stream gradients.
5	Pliocene	Formation of the Bet-Kerem half-graben structure.	$1.8–2.0 \times 10^{11}$	300–350	0	Isostatic uplift due to tectonic unloading
6	Early Pleistocene to recent	Arching and formation of main water divide (Matmon et al., 1999)		150–200	0	Bet-Kerem structure is on arch axis. Carmel structure is not
Total calculated topographic contributions				550–750	125–200	
Total calculated topographic difference between Carmel and Upper Galilee blocks				350–625		
Observed topographic elevations				900–1000	450–550	
Total observed topographic difference between Carmel and Upper Galilee blocks				350–550		

5.2. Evolutionary model

We use the described processes above to explain, in a semi-quantitative model, the development of the Carmel and the Upper Galilee half-grabens and the elevation differences that developed between them.

5.2.1. Stage 1—Pre-Miocene

In the early Miocene, the study area consisted of short wavelength (10–20 km wide) synclines and anticlines of the Syrian Arc fold belt, which were truncated to a low relief morphology during the Oligocene (Fig. 6A; Table 2).

5.2.2. Stage 2—Early Miocene

The southern half-graben unit started developing in the early Miocene (Fig. 6B; Table 2). The formation of the half-graben caused a local mass deficit, which was followed by isostatic uplift along the Carmel Fault. In order to calculate the isostatic uplift we use an elastic plate model following the formulations of Turcotte and Schubert (1982). The model, which is applied to long and narrow linear features, such as fault systems, assumes an infinitely, long elastic plate that bends upward (or downwards) in response to an infinitely long, uniform load (line-load) applied along the linear feature. The above assumptions reduce the mathematical problem to one dimension-distance normal to the fault. This widely used model (e.g., King et al., 1988; Ebinger et al., 1991; Wdowinski and Zilberman, 1996) depends on three parameters: the plate's Young's modulus, its elastic thickness, and the magnitude of the applied line-load.

King et al. (1988), who studied the growth of local geological structures by repeated earthquake, concluded that fault structures are associated with apparent elastic thickness of 4 km or less, suggesting a very low flexural rigidity of the crust. The elastic thickness parameter predominantly determines the width of uplifted area, which in case of 4 km thickness is 60 km wide (King et al., 1988). Using the reported 4-km elastic thickness, Young's modulus of 2.5×10^{10} N m^{-2} (King et al., 1988), we need only to calculate the line-load in order to estimate the amplitude of maximum uplift or subsidence.

We calculate from the southern half-graben shape (Fig. 7) a line-load of $1.7–2 \times 10^{11}$ N m^{-1} (Table 2) and, hence, estimate maximum isostatic uplift of 300–350 m. Using the same formulations and param-

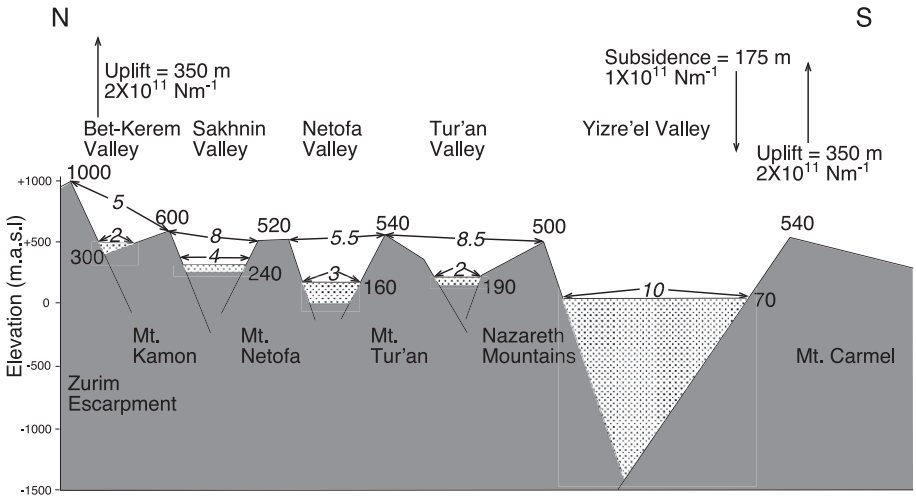

Fig. 7. Schematic cross-section from top of Zurim Escarpment to Mt. Carmel through the central part of the Lower Galilee. This figure is used to calculate the line-load across the two half-graben units. The magnitude of the applied load was derived by assuming simple two-dimensional geometric shapes (triangular, trapezoid, or rectangular) of the valley fills and calculating their areas. For simplicity, any of the inner lower Galilee faults were not marked. Italic numbers—valley widths and distances between peaks (km). Plain numbers—elevation above sea level (m) of valley floors and peaks. Horizontal axis is not to scale.

eters, we calculate that the sediment line-load in the Yizre'el Valley is $0.8–1.0 \times 10^{11}$ N m^{-1} (Table 2), causing a maximum subsidence of 150–175 m, half of the uplift value. Thus, the total uplift of the Carmel morpho-structural unit due to isostatic response was about 150–175 m.

As a result of the subsidence of the Yizre'el Valley, a drainage system that drained the Galilee southward into the Yizre'el Valley developed (Fig. 6B, Kafri, 1997). This implies that the northern Lower Galilee was 100–200 m higher than the Yizre'el Valley (if considering a 0.5% alluvial gradient) when later faulting that formed the northern boundary half-graben and other blocks in the Lower Galilee begun operating.

5.2.3. Stage 3

A second isostatically supported half-graben morpho-structural unit started developing in the Pliocene across the Bet-Kerem Fault system in response to a N–S extensional stress field. Synthetic and antithetic normal faults developed within the down flexed hanging wall and formed the horst and graben morphology of the Lower Galilee (Fig. 6C). We calculate from the northern half-graben shape a line-load of $1.7–2 \times 10^{11}$ N m^{-1} (Fig. 7, Table 2) and, hence, estimate maximum isostatic uplift of 300–350 m. The insignificant sedimentary loading in the northern valleys resulted in a negligible basin subsidence.

The arching of the western margins of the DSF (Wdowinski and Zilberman, 1997) caused the uplift of the mountain ranges along an N–S axis. In the Galilee, the arching contributed about 150–200 m of elevation during the Pleistocene (Matmon et al., 1999). The axis of the N–S trending arch crosses the Bet-Kerem Fault and, thus, influences it and the upper Galilee block. However, the Carmel block lies west of the axis, and was only marginally influenced by this regional uplift (Fig. 6C).

Together, the total contribution to the elevation of the Carmel structure from the isostatic compensation, regional tilt, and arching is 125–200 m while for the Bet-Kerem structure it is 550–750. The processes described above and summarized in Table 2 explain the difference in topographic elevation between the two uplifted margins in spite of their similar vertical displacement.

6. Discussion

The results of our study show that the present structure and morphology of the Galilee were formed by the development of two half-graben units. The southern one started developing in the early Miocene and the northern one in the Pliocene. Although both boundary blocks are similar in many aspects such as the amount of stratigraphic displacement and isostatic uplift (calculated in our model), the two boundary faults of the extending region differ from one another in their orientation, topographic elevation, and structural elevation. In this section, we discuss the causes for the observed differences and also provide explanations for the causes.

The two boundary fault systems, the older Carmel Fault and the younger Bet-Kerem Fault, are oriented at 45° to one another. The older Carmel Fault is oriented NW–SE, whereas the younger Bet-Kerem Fault is oriented E–W. This observed orientation difference was caused by the varying stress field that shaped the Galilee and the entire Levant structures (Eyal and Reches, 1983; Ron and Eyal, 1985; Eyal, 1996). Since the Miocene, the region was subjected to predominantly extensional stress field associated with the breakup of the Arabo–Nubian plate. The formation of the Carmel Fault during an early Miocene rifting period occurred contemporaneously to the formation of the Red Sea and the Gulf of Suez (which are sub-parallel to the Carmel Fault) in response to an ENE–WSW regional extensional stress field (Garfunkel, 1981). However, during the middle and late Miocene transcurrent faulting occurred throughout the Levant forming the DSF under ENE–WSW extension and NNW–SSE compression. Throughout the Galilee, a local stress-field of E–W compression and N–S extension generated left lateral displacement along the Carmel Fault and formed NE–SW right-lateral trending faults and their conjugate NW–SE left-lateral trending faults (Ron and Eyal, 1985). Since the Pliocene, the E–W compressional component of the stress-field has been significantly reduced; thus the Galilee has been subjected to N–S extension occurring along E–W normal faults (Ron and Eyal, 1985) and a broad E–W folding, the arching. Thus, the 45° orientation difference between the northern and southern boundary faults of the Lower Galilee is, therefore, the result of the different stress fields under which each fault developed.

Although the shallow structure of both fault systems is similar along the opposite facing half-grabens, the Galilee deep structure reflects significant differences. The deep structure of the Lower Galilee has been interpreted from magnetic and gravimetric anomaly maps (e.g., Ginzburg, 1970; May, 1987; Shirman, 2000; Rybakov et al., 2000). May (1987) pointed out that the gravimetric signal north of the Carmel Fault generally rises from east to west towards the Mediterranean. This phenomenon, which was not observed south of the Carmel Fault, apparently stems from a thinner crust north of the Carmel Fault compared to the crust south of it indicating a change in crust properties along the Carmel line (Ginzburg et al., 1994). The positive gravimetric anomaly along the length of the Carmel Fault of about 30 to 35 mGal was interpreted as either representing the existence of an intrusive body at a depth of 3–5 km or by the deformation of the basement by the deep Carmel Fault (May, 1987; Hofstetter et al., 1996). May (1987) pointed to the fact that the block structure of the Lower Galilee is not expressed in the gravimetric and magnetic fields and explained this by low angle listric faults that do not penetrate the basement and therefore do not form anomalies. He suggested that the extensional domain of the Lower Galilee is bounded in the south by the deep Carmel Fault and in the north by the main listric fault of Bet-Kerem (Fig. 8).

Minor seismic activity in the Galilee and moderate seismic activity along the Carmel Fault also shed light on the differences between the two fault systems and basically support May's (1987) deep structure interpretation. Based on an analysis of the seismic activity in the eastern Mediterranean area, Salamon et al. (1996) suggested the Carmel Fault is part of the present northern boundary of the rigid portion of the Sinai subplate. Hofstetter et al. (1996) suggested that the western boundaries of the DSF comprise of two micro-plates, separated by the Carmel Fault: the southern micro-plate includes all of Israel south of the Carmel Fault and the northern micro-plate includes northern Israel and Lebanon.

The difference in the geometry of the boundary faults can help to explain the differences in the morphologic and structural elevations of the half-grabens and the amount of sediment that accumulated in them. The deep Carmel Fault enabled the significant subsidence of the adjacent half-graben, the Yizre'el Valley. The subsidence created a low base level that accumulated sediments from a large drainage basin in the north that included most of the Lower Galilee (Kafri, 1997). In contrast, the listric Bet-Kerem fault that, according to May (1987) flattens at shallow depths within the sedimentary sequence did not enable significant subsidence, therefore not inducing the accumulation of a thick sedimentary sequence. Furthermore, the development of the Bet-Kerem listric fault was accompanied by the development of the E–W oriented structural blocks in the Lower Galilee during the Pliocene. As a result, the region was split into small drainage basins that flowed westward to the Mediterranean or eastward to the Dead Sea Valley between the Lower Galilee uplifted blocks. The breakup of the Lower Galilee into small uplifted blocks caused transport to and accumu-

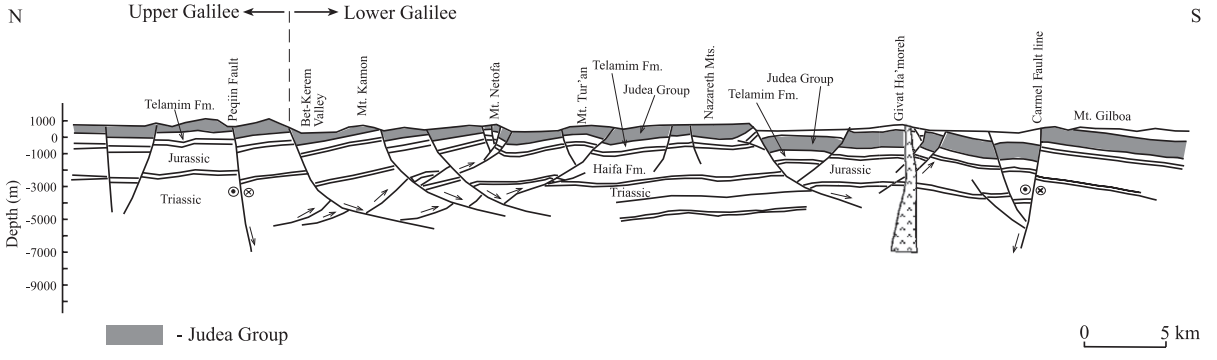

Fig. 8. The deep structure of the Galilee modified after May (1987). The extensional structure of the Galilee is bounded in the south by the deep Carmel Fault that penetrates the crust and in the north by the main listric Bet-Kerem Fault system. The various blocks in the Lower Galilee are bounded by secondary listric faults.

lation of sediments in the Yizre'el Valley to decrease significantly and did not enable the accumulation of sediment in the Bet-Kerem Valley.

The absolute topographic elevation of the boundary blocks is dictated by several factors such as their location relative to regional uplift axis and the absolute amount of displacement along the Bet-Kerem and Carmel faults. Our model cannot explain the absolute elevations of each of the blocks since there are no markers to signify surface uplift in the region (England and Molnar, 1990; Molnar and England, 1990). However, the model can explain the difference in elevation between the two boundary blocks.

The elevation differences between the northern and southern bounding blocks can be explained considering several factors (Table 2): (1) Elevation differences that existed during the time interval between the formation of the southern half-graben and the northern one (Fig. 6B). (2) The influence of the N–S trending structural arch that formed the mountainous backbone of Israel (Fig. 6C). (3) Difference in isostatic compensation due to sedimentary loading (Fig. 6). The combination of the elevation contribution of the described processes helps to explain the differences in structural and topographic elevations between the two boundary half-grabens and blocks of the Lower Galilee. We calculated similar amounts of isostatic uplift as response to normal faulting along the Bet-Kerem faults system and the Carmel Fault. However, the uplift was enhanced along the Bet-Kerem faults system by regional arching, and negated along the Carmel Fault by substantial loading of sediments in the Yizre'el Valley. Thus, according to the model calculations, an elevation difference of 350–625 (average, ~ 485) m should develop between the boundary blocks. This value agrees with the actual difference of 350–550 (average, ~ 450) m between the Carmel Block and top of Zurim Escarpment.

7. Conclusions

The results of our study suggest that the morphologic and tectonic history of the Lower Galilee, the Yizre'el Valley, and their adjacent bounding blocks are best described by a set of two opposite facing half-grabens. Total extension in the Galilee was achieved by the formation of two half-grabens under varying stress fields. The formation of the southern half-graben during the Miocene occurred under a stress field related to the opening of the Red Sea and the Gulf of Suez (and other basins in the region). The subsidence of the half-graben along the deep-seated Carmel Fault formed the Yizre'el Valley. The drainage basin of the Yizre'el Valley was extensive and enabled the delivery and accumulation of sediments into the valley. As a consequence, the isostatic uplift of the half-graben unit was negated by subsidence caused by sedimentary load.

The second, northern half-graben was formed along the listric Bet-Kerem fault system during the Pliocene and occurred under a stress field related to the development of the DSF. The development of the block structure within the Lower Galilee occurred at this time and several small drainage systems developed between the uplifted blocks. Thus, only little sedimentary accumulation could take place in the northern half-graben. Furthermore, the extensive drainage basin that transported sediments to the Yizre'el Valley was significantly reduced and sediment accumulation rate decreased. The shallow listric fault that formed the northern boundary did not cause significant subsidence and the small drainage basins did not transport substantial amounts of sediments to the northern half-graben. Thus, the isostatic uplift of the northern half-graben unit was not followed by accumulation of sediments and subsidence.

In summary, the two half-grabens differ from one another by their orientation, structural and topographic elevation. The southern half-graben is deeper, exceeds to a depth of 1500 m, and is filled with Miocene–Pliocene sediments and volcanic rocks. The northern half-graben exceeds up to 800 m of vertical offset and is hardly filled with sediments. However, the northern uplifted block is topographically higher by 400–600 m than the southern one. The differences between the two half-grabens are attributed to original elevation differences, the thick fill of volcanics and sediments along the southern half-graben, and the influence of arching on the northern half-graben.

Acknowledgements

We thank P. Bierman, K. Nichols, S. Hurwitz, and S. Marco for collegial reviews of early drafts of the

manuscript, and Z. Garfunkel and A. Agnon for fruitful discussions and ideas. We are thankful to two anonymous reviewers for their helpful comments.

References

Achmon, M., 1986. The Carmel border fault between Yoqneam and Nesher (in Hebrew, English abstract). MSc thesis, Hebrew University of Jerusalem, Jerusalem. 56 pp.

Achmon, M., Ben-Avraham, Z., 1997. The deep structure of the Carmel Fault zone, northern Israel, from gravity field analysis. Tectonics 16 (3), 563–569.

Avni, Y., 1990. The paleogeography and the evolution of the landscape in the western part of the central Negev, and the relationship to the evolution of Makhtesh–Ramon. In: Lavee, H., Schick, A., Yair, A. (Eds.), Facets of the Geomorphology of the Negev. The Israel Geomorphological Society, pp. 67–84.

Avni, Y., 1991. The geology, paleogeography and landscape evolution of the Negev highlands and the western Ramon structure. Geological Survey of Israel, Report GSI/6/91. 153 pp.

Ball, M.H., Ball, D., 1953. Oil prospects of Israel. Bulletin of American Association of Petroleum Geologists 37, 1–113.

Begin, Z.B., Zilberman, E., 1997. Main stages and rates of relief development in Israel. Geological Survey of Israel, Report GSI/24/97. 63 pp.

Belitzki, S., 1997. Tectonic geomorphology of the lower Jordan Valley—an active continental rift (in Hebrew with extended English abstract). PhD Thesis, Hebrew University of Jerusalem, Jerusalem. 98 pp.

Ben-Gai, Y., Ben-Avraham, Z., 1995. Tectonic processes in offshore northern Israel and the evolution of the Carmel structure. Marine and Petroleum Geology 12, 533–548.

Bentor, Y.K., Vroman, A.J., 1951. Map of the Negev. Sheet 18: Avedat, scale 1:100,000, Israel Army SCI. 98 pp.

Bentor, Y.K., Vroman, A.J., 1961. Map of the Negev. Sheet 16: Mt. Sedom, scale 1:100,000, Israel Army SCI. 98 pp.

Cohen, Z., 1988. Hydrocarbon Potential of Israel, Highlights of Basin Analysis. Oil Exploration in Israel Ltd., Exploration Department. 79 pp.

Dvorkin, A., Kohn, B.P., 1989. The Asher Volcanics, northern Israel: petrography, mineralogy and alteration. Israel Journal of Earth Sciences 38, 105–123.

Ebinger, C.J., 1989. Tectonic development of the western branch of the East African rift system. Geological Society of America Bulletin 101, 885–903.

Ebinger, C.J., Rosendahl, B.R., Reynolds, D., 1987. Tectonic model of the Malawi rift, Africa. Tectonophysics 141, 215–235.

Ebinger, C.J., Karner, G.D., Weissel, J.K., 1991. Mechanical strength of extended continental lithosphere: constraints from the western rift system, east Africa. Tectonics 10, 1239–1256.

Eliezri, I.Z., 1965. The geology of the Beit–Jann region (Galilee, Israel). Israel Journal of Earth Sciences 14, 51–66.

Ellenblum, R., Marco, S., Agnon, A., Rockwell, T., 1998. Crusader castle torn apart by earthquake at dawn, 20 May, 1202. Geology 26 (4), 303–306.

England, P., Molnar, P., 1990. Surface uplift, uplift of rocks, and exhumation of rocks. Geology 18, 1173–1177.

Eyal, Y., 1996. Stress field fluctuations along the Dead Sea Rift since the middle Miocene. Tectonics 15 (1), 157–170.

Eyal, Y., Reches, Z., 1983. Tectonic analysis of the Dead Sea Rift region since the Late Cretaceous based on mesostructures. Tectonics 2 (2), 167–185.

Flexer, A., Freund, R., Reiss, Z., Buchbinder, B., 1970. Santonian paleostructure of the Galilee. Israel Journal of Earth Sciences 19, 141–146.

Freund, R., 1965. A model of the structural development of Israel and adjacent areas since Upper Cretaceous times. Geology Magazine 102, 189–205.

Freund, R., 1970. The geometry of faulting in Galilee. Israel Journal of Earth Sciences 19, 117–140.

Garfunkel, Z., 1970. The tectonics of the western margins of the southern Arava (in Hebrew, English abstract). PhD thesis, Hebrew University of Jerusalem, Jerusalem. 204 pp.

Garfunkel, Z., 1978. The Negev—regional synthesis of sedimentary basins. Tenth International Congress of Sedimentology, Jerusalem, Guidebook to Excursions 1, 33–110.

Garfunkel, Z., 1981. Internal Structure of the Dead Sea leaky transform (rift) in relation to plate kinematics. Tectonophysics 80, 81–108.

Garfunkel, Z., 1988. The pre-Quaternary geology of Israel. In: Yom-Tov, Y., Tchernov, E.W. (Eds.), The Zoogeography of Israel. Junk, The Hague, Netherlands, pp. 7–34.

Garfunkel, Z., Horovitz, A., 1966. The Upper Tertiary and Quaternary morphology of the Negev. Israel Journal of Earth Sciences 15, 101–117.

Garfunkel, Z., Derin, B., 1984. Permian–early Mesozoic tectonism and continental margin formation in Israel and its implications for the history of the eastern Mediterranean. In: Dixon, J.E., Robertson, A.H.F. (Eds.), The Geological Evolution of the Eastern Mediterranean. Geological Society Special Publication, vol. 17, pp. 187–201.

Garfunkel, Z., Almagor, G., 1985. Geology and structure of the continental margin off northern Israel and the adjacent part of the Levantine basin. Marine Geology 62, 105–131.

Garfunkel, Z., Ben-Avraham, Z., 1996. The structure of the Dead Sea Basin. Tectonophysics 266, 155–176.

Ginzburg, A., 1970. The Gravity Map of Israel. Atlas of Israel, 2nd ed. Survey of Israel, Jerusalem and Elsevier, Amsterdam.

Ginzburg, A., Ben-Avraham, Z., Makris, J., Hubral, P., Rotstien, Y., 1994. Crustal structure of northern Israel. Marine and Petroleum Geology 11 (4), 501–506.

Glikson, Y.A., 1966. Geology of the Southern Naftali Mountains (northeastern Galilee, Israel). Israel Journal of Earth Sciences 15, 135–154.

Golani, U., 1957. The Geology of the Meghar region (in Hebrew). MSc thesis, Hebrew University of Jerusalem, Jerusalem. 54 pp.

Gran-Mitchel, S.E., Matmon, A., Bierman, P.R., Rizzo, D., Enzel, Y., Caffee, M., 2001. Determination of displacement history from a limestone normal fault scarp using cosmogenic ^{36}Cl, northern Israel. Journal of Geophysical Research 106 (B3), 4247–4264.

Hall, J.K., 1993. The GSI digital terrain model (DTM) project

completed. Geological Survey of Israel Current Research 8, 47–50.

Hall, J.K., 1996. Topography and bathymetry of the Dead Sea depression. Tectonophysics 266, 177–185.

Heimann, A., 1990. The development of the Dead Sea Transform and its margins in northern Israel during the Pliocene and Pleistocene (in Hebrew, English summary). Geological Survey of Israel, Report GSI/28/90. 83 pp.

Hofstetter, A., Van-Eck, T., Shapira, A., 1996. Seismic activity along branches of the Dead Sea–Jordan Transform system: The Carmel–Tirtza fault system. Tectonophysics 267, 317–330.

Hurwitz, S., Garfunkel, Z., Ben-Gai, Y., Reznikov, M., Rotstein, Y., Gvirtzman, H., 2002. The tectonic framework of a complex pull-apart basin; seismic reflection observations in the Sea of Galilee, Dead Sea Transform. Tectonophysics 359, 289–306.

Issar, A., Kafri, U., 1972. Neogene and Pleistocene Geology of the Western Galilee Coastal Plain. Geological Survey of Israel Bulletin 53. 14 pp.

Kafri, U., 1972. The geological map of Israel, Nahariyya. Geological Survey of Israel, Ministry of Development, State of Israel, scale 1:50,000, Sheet 1-IV.

Kafri, U., 1997. Neogene to Quaternary drainage systems and their relationship to young tectonics: Lower Galilee, Israel. Geological Survey of Israel, Report GSI/1/97. 50 pp.

Kafri, U., Ecker, A., 1964. Neogene and Quaternary subsurface geology and hydrology of the Zevulun Plain. Geological Survey of Israel Bulletin 37. 13 pp.

Karcz, Y., 1959. The structure of the northern Carmel. Bulletin of the Research Council of Israel 80G, 119–130.

Kashai, E., Picard, L., 1958. On the lithostratigraphy and tectonics of the Carmel. Bulletin of the Research Council of Israel 7G (1), 1–19.

King, G.C., Stein, R.S., Rundle, J., King, B., 1988. The growth of geological structures by repeated earthquakes: 1. Conceptual framework. Journal of Geophysical Research 93 (11), 13307–13318.

Krenkel, E., 1924. Der Syrische Bogen. Zentralblatt Mineralogie 9, 274–281.

Levy, Y., 1983. The geological map of Israel, Shefar'am. Geological Survey of Israel, Ministry of Development, State of Israel, scale 1:50,000, Sheet 3-II.

Marco, S., Agnon, A., Ellenblum, R., Eidelman, A., Basson, U., Boas, A., 1997. 817 year old walls offset sinistrally 2.1 m by the Dead Sea Transform, Israel. Journal of Geodynamics 24 (1–4), 11–20.

Matmon, A., Enzel, Y., Zilberman, E., Heimann, A., 1999. Late Pliocene and Pleistocene reversal of drainage systems in northern Israel: tectonic implications. Geomorphology 28, 43–59.

Matmon, A., Zilberman, E., Enzel, Y., 2000. Determination of escarpment age using morphologic analysis: an example from the Galilee, northern Israel. Geological Society of America Bulletin 112 (12), 1864–1876.

May, P.R., 1987. Oil and Gas Potential of the Galilee, Israel, Report 87/12. Oil Exploration of Israel Ltd., Exploration Department. 79 pp.

Mero, D., 1983. Subsurface geology of western Galilee and Zevulun plain. Tahal Consulting Engineering Ltd.

Molnar, P., England, P., 1990. Late Cenozoic uplift of mountain ranges and global climate change: chicken or egg? Nature 346 (6279), 29–34.

Mor, D., Levitte, D., Steinitz, G., Lang, B., 1987. The volcanic history of the Ramat Dalton (Upper Galilee) according to K–Ar dating. Israel Geological Society, Annual Meeting, 93.

Nir, D., 1970. Geomorphology of Israel. Aqademon, Jerusalem, Israel. 404 pp.

Picard, L., 1943. Structure and evolution of Palestine with comparative notes on neighboring countries. Hebrew University, Jerusalem, Geological Department Bulletin 4. 134 pp.

Picard, L., 1951. Geomorphogeny of Israel. Part 1—The Negev. The Bulletin of the Research Council of Israel 8G, 1–30.

Picard, L., Golani, U., 1965. The Geological Map of Israel, Northern Sheet, 1:250,000, Mapping Division, Israel.

Quennell, A.M., 1959. Tectonics of the Dead Sea rift. 20th International Geological Congress. Association of Surveying Geologists, Africanos, Mexico, pp. 385–405.

Ron, H., Eyal, Y., 1985. Interplate deformation by block rotation and mesostructures along the Dead Sea Transform, northern Israel. Tectonics 4 (1), 85–105.

Ron, H., Freund, R., Garfunkel, Z., Nur, A., 1984. Block rotation by strike slip faulting: structural and paleomagnetic evidence. Journal of Geophysical Research 89, 6256–6270.

Rosendahl, B.R., 1987. Architecture of continental rift with special reference to East Africa. Annual Review of Earth Planetary Sciences 15, 445–503.

Rybakov, M., Goldshmidt, V., Fleischer, L., Ben-Gai, Y., 2000. 3-D gravity and magnetic interpretation for the Haifa Bay area (Israel). Journal of Applied Geophysics 44, 353–367.

Salamon, A., 1987. The monoclines in the northern Negev: a model of tilted blocks and shortening (in Hebrew with English abstract). MSc thesis, Hebrew University of Jerusalem, Jerusalem. 101 pp.

Salamon, A., Hofstetter, A., Garfunkel, Z., Ron, H., 1996. Seismicity of the eastern Mediterranean region: perspective from the Sinai subplate. Tectonophysics 263, 293–305.

Saltzman, U., 1964. The geology of the Tabha–Huquq–Migdal area (in Hebrew). MSc thesis, Hebrew University of Jerusalem, Jerusalem. 55 pp.

Schulman, N., 1959. The geology of the Central Jordan Valley. Bulletin of the Research Council of Israel 8G, 63–90.

Schulman, N., 1962. The geology of the Central Jordan valley (in Hebrew). PhD thesis, Hebrew University of Jerusalem, Jerusalem. 103 pp.

Shaliv, G., 1991. Stages in the tectonic and volcanic history of the Neogene basin in the Lower Galilee and the valleys. Geological Survey of Israel, Report GSI/11/91. 101 pp.

Shirman, B., 2000. Three component magnetic anomaly maps of Israel. Israel Journal of Earth Sciences 49, 1–7.

Sivan, D., 1996. Paleogeography of the Galilee coastal plain during the Quaternary (in Hebrew). Geological Survey of Israel, Report GSI/18/96. 228 pp.

Sivan, D., Gvirtzman, G., Sass, E., 1999. Quaternary stratigraphy and paleogeography of the Galilee Coastal Plain. Quaternary Research 51, 280–294.

ten Brink, U.S., Schoenberg, N., Kovach, R.L., Ben-Avraham, Z., 1990. Uplift and possible Moho offset across the Dead Sea transform. In: Kovach, R.L., Ben-Avraham, Z. (Eds.), Geologic and Tectonic Processes of the Dead Sea Transform Zone. Tectonophysics, vol. 180, pp. 71–85.

Turcotte, D.L., Schubert, G., 1982. Geodynamics, Application of Continuum Physics to Geological Problems. Wiley, New York. 450 pp.

Wdowinski, S., Zilberman, E., 1996. Kinematic modeling of large scale structural asymmetry across the Dead Sea Transform. Tectonophysics 266, 187–201.

Wdowinski, S., Zilberman, E., 1997. Systematic analyses of the large-scale topography and structure across the Dead Sea Rift. Tectonics 16, 409–424.

Wernicke, B.P., 1981. Low-angle normal faults in the Basin and Range province: nappe tectonics in an extending orogen. Nature 291, 645–648.

Wernicke, B.P., Burchfield, B.C., 1982. Modes of extensional tectonics. Journal of Structural Geology 4, 105–115.

Zilberman, E., 1992. Remnants of Miocene landscape in the central and northern Negev and their paleogeographic implications. Israel Geological Survey Bulletin 83. 54 pp.